Analyst

ROYAL SOCIETY OF CHEMISTRY

PAPER

View Article Online
View Journal | View Issue

Cite this: *Analyst*, 2023, **148**, 5178

Fluorescent fiber-optic device sensor based on carbon quantum dot (CQD) thin films for dye detection in water resources†

Tanmay Vyas,[a] Manashjit Gogoi [b] and Abhijeet Joshi *[a]

Industrialization, especially in textile industries, has led to increased use of dyes and pigments to impart colours to fabrics. Textile dyes are one of the chief emerging pollutants of water resources as industrial effluents. In the current research, we report the development and utilization of pH-sensitive carbon quantum dots (CQDs) immobilized in polymer thin films acting as sensors for textile dye detection. The CQDs and CQD-containing polymer films were characterized by various techniques like XRD, TEM, XPS, and CLSM. The synthesized CQD thin films possess a unique pH-sensitive property that can be used to detect various model acidic and basic dyes that are important components of industrial effluents from textile dyes. The detection capability of the sensor films was evaluated by spiking dyes in various water matrices, like household tap water and river water. The results indicate that pH-sensitive CQD thin film was able to detect three acidic dyes, namely methyl red, methyl orange, and bromocresol green, and one basic dye, methylene blue, in a linear range of 0–100 μM with a response time of 1 minute. The CQD thin-film sensors have a limit of detection of 26.4 ppb, 214.5 ppb, 46.2 ppb, and 29.7 ppb for methyl red, methyl orange, bromocresol green and methylene blue, respectively. The accuracy of detection performed by spiking studies in water resources indicated an ~100% recovery value in all tested acidic and basic dyes. The sensor films were compared for analytical parameters using UV-visible-fluorescence spectroscopy and HPLC.

Received 4th August 2023,
Accepted 29th August 2023

DOI: 10.1039/d3an01343j

rsc.li/analyst

1. Introduction

Industrialization and urbanization of society have led to significant amounts of contamination of the environment. Extensive use of synthetic and chemical-based compounds like volatile organic compounds (VOCs), pesticides, dyes, antibiotics, *etc*. means these compounds become the main pollutants in various water resources. Among them, synthetic dyes are chemical compounds used to impart colours to fibres of textiles due to their simple attachment capabilities. Dyes are synthetic and/or natural molecules that are used in industries for imparting colours on clothes (textiles), medicines, leather, food, and paper products.[1] Sustainability, wide availability, and cost-effectiveness make synthetic dyes more preferred over natural dyes. Around 10 thousands varieties of dyes are present in the marketplace having production costs of more than 1 million annually.[2] Based on the functional groups of the molecular structure, dyes are classified into azo, indigo, vat, nitro, anthraquinone, carbonium, *etc*.[4] Dyes are also classified into various groups on the basis of solubility, structure, *etc*. According to solubility, dyes are classified into acidic, dispersed, reactive, and basic dyes.[3] Methyl red is a benzoic and diazinyl group-based acidic dye that is mainly used in the textile and paper industries.[5] Similarly, acidic dyes like bromocresol green (triphenyl methane based), methyl orange (anionic azo dye), and basic dyes like methylene blue (cationic thiazine) are used in paper, textile, and cotton industries mainly to impart colour.[6] The permissible limits of these vary from dye to dye in the range of 1–16 ppm[7] above which the dyes cause several toxic effects on the environment, mainly water pollution[8] and soil pollution.[9] Several health issues have been reported when human beings are exposed, such as conformational changes and damage in DNA,[10] neurotoxic effects,[11] diarrhoea, allergies and hepatotoxicity,[7] eye and skin irritation,[12] vomiting, jaundice and abdominal issues,[13] carcinogenic effects,[14] *etc*. Due to the occurrence of all these severe

[a]*Department of Biosciences and Biomedical Engineering, Indian Institute of Technology Indore, Khandwa Road, Indore-453552, Madhya Pradesh, India. E-mail: abhijeet.joshi@iiti.ac.in; Tel: +91-731-6603344*
[b]*Department of Biomedical Engineering, North-Eastern Hill University, Umshing Mawkynroh, Shillong 793022, India*

† Electronic supplementary information (ESI) available. See DOI: https://doi.org/10.1039/d3an01343j

and hazardous effects on health and the environment, detection of dyes in natural matrices is an essential concern for devising strategies for their degradation and treatment.

Various classical techniques and instruments have been used for the detection of dyes, such as high performance liquid chromatography,[15] column chromatography,[16] ion mobility spectrometry,[17] derivative spectrophotometry,[18] Raman spectroscopy,[19] capillary electrophoresis,[20] *etc*. All these classical techniques have the ability to detect dyes with good sensitivity, accuracy and specificity but have many disadvantages like high cost, being non-portable in nature, requiring pre-sample treatment, being time consuming, and involving complicated data analysis.[21] A strong requirement exists for the development of a unique method that can eliminate these disadvantages and provide the possibility of a point-of-care approach.

Several studies have been using fluorescence-based approaches for the detection of various environmental analytes like volatile organic compounds (VOCs),[22] heavy metals,[23] dyes[24] and pesticides.[25]

Fluorescence-based techniques rely on many fluorescent probes, like fluorescent dyes, quantum dots (QDs), and metal organic frameworks (MOFs), for the detection of analytes in complex matrices. Quantum dots have unique fluorescence properties due to which they are gaining attention for the development of assays based on fluorescence and have many advantages as compared to other fluorophores, including high photostability, better fluorescence time, and narrow emission and broad excitation. QDs can also undergo a variety of mechanisms such as fluorescence resonance energy transfer (FRET), fluorescence, energy transfer, luminescence, photocurrent generation, *etc*.[26–28] Carbon quantum dots (CQDs) have additional advantageous properties such as biocompatibility, biological tunability, non-toxicity, cost effectiveness *etc*. With these additional properties CQDs are capable of being used in various biological applications where the biggest concern is toxicity.[29,30]

Use of carbon dots for the detection of dyes is meagre in the literature and the methods all have the disadvantages of non-portability, complex mechanisms, use of laboratory-scale instruments and requirement of improvement of several analytical parameters like real-time monitoring, sensitivity, specificity, limit of detection *etc*. when simple mechanisms are used.

Carbon quantum dots are used as sensing platforms for the detection of various textile dyes that involve various sensing strategies like the inner filter effect mechanism associated with tyre-derived carbon to detect Sudan dyes I, II, III, and IV with LODs of 0.17, 0.21, 0.62, and 0.53 μM, respectively.[31] In another study sulphuric acid-mediated red-emission-based carbon dots that were N, S codoped were used in the detection of food dyes, such as methylene blue, amaranth and brilliant blue with LODs of 4 nM, 70 nM, and 20 nM, respectively, along with cell imaging.[32] The iodide dyes were selectively detected through carbon dots by a quenching mechanism with an LOD of 430 nM in the range of 0.5–20 μM.[33]

In the current study, carbon quantum dot (CQD)-loaded polymeric thin films were synthesized with the objective of a point-of-care approach for detection using a fiber-optic spectrometer. CQD thin films were characterized for various properties like elemental, optical, structural and morphological properties. The pH-sensitive response of the synthesized CQD thin films was used to detect various acidic and basic textile dyes (methyl red, methyl orange, methylene blue, bromocresol green) in water matrices through a spiking study. Analytical parameters like limit of detection, sensitivity, accuracy, specificity and response time were evaluated for the thin-film sensor and compared against the HPLC-based method of detection.

2. Materials and methods

2.1 Materials

Folic acid (MW 441.40 g mol^{-1}) was procured from SRL PVT. Ltd, India. All dyes, namely methyl red, methyl orange, methylene blue and bromocresol green, were purchased from Hi-Media, India. Acetonitrile and methanol were procured from Thermo Fisher, India. All solvents and chemicals used were of HPLC grade and double-distilled water was used for all working solutions, buffers, and synthesis of carbon quantum dots.

2.2 Synthesis of carbon quantum dots (CQDs) and immobilization to form CQD-containing thin films

Folic acid (22.6 M) was obtained in double-distilled water for the preparation of CQDs. The solution was kept in a hot-air oven at 180 °C for 2 hours (Fig. 1) and then allowed to cool to room temperature. The synthesized CQD solution was purified by filtration with 0.2 μm nylon filter rings as CQDs have sizes ranging between 1 and 10 nm and, after filtration, the filtered solution was dialyzed in 15 ml of double-distilled water. Powder CQDs are formed by lyophilizing the dialyzed samples. Thin films containing CQDs were developed using 5% w/v chitosan obtained in 35 mL of DI water. The synthesized CQD suspension was poured into Petri plates and allowed to solidify at room temperature. The thin films of CQDs prepared were cut into smaller discs using a paper punching cutter having an approximate diameter of 3–5 mm.

2.3 Characterization of folic acid CQD loaded thin films

The chemical composition of the synthesized thin film of CQDs was analysed using X-ray photoelectron spectroscopy (XPS) (beamline PES-BL-14). For the analysis of crystalline and lattice parameters, X-ray diffraction (XRD) was performed using a CuKα X-ray source (1.54 Å) (Rigaku Smart Lab). The morphological characterization and size distribution of the synthesized CQDs were analysed by transmission electron microscopy (TEM) (model CM 20, Philips India), where a copper grid was used to drop cast CQDs for TEM. The chemical nature and functional group identification of the synthesized CQD thin film were acquired using Fourier transform

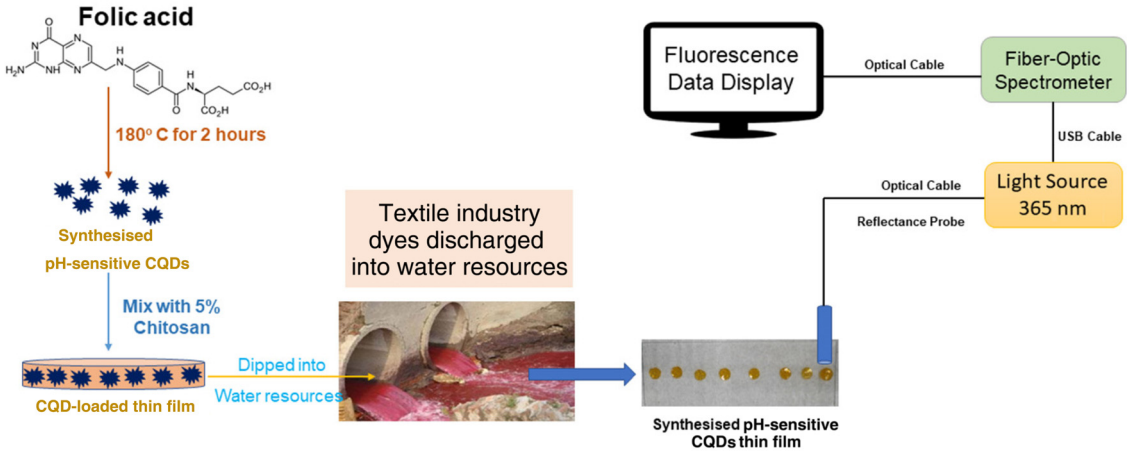

Fig. 1 Schematic diagram of the synthesis of CQDs and work plan of investigation.

infrared spectroscopy (FTIR) (Tensor 27, Bruker, Germany) in the range 4000–400 cm^{-1}. The optical characterization and absorbance of the CQDs were observed in a UV-vis spectrophotometer (Shimadzu, UV1900i, Japan) and the fluorescence of CQDs was observed in a fiber optic spectrophotometer (FOS) device (Flame, Ocean Optics, Denmark). Confocal laser scanning microscopy (CLSM) (IX, Olympus, Japan) was performed for the evaluation of the distribution of fluorescence obtained from CQDs in the thin film. For the evaluation of quantum yield, quinine sulphate dye was used as the reference and absorption of quinine sulphate and CQD solution was measured along with the emission intensity of the CQD solution and calculated using the following formula:

$$\text{Quantum yield} = \text{QY of dye} \times \frac{\text{Abs of dye}}{\text{Abs of CQDs}} \times \frac{\text{intensity of CQDs}}{\text{intensity of dye}}$$

2.4 Evaluation of pH response of synthesized CQD thin films

The pH response of the CQD thin film was evaluated by exposing the CQD thin film to different pH buffers from pH 3 to pH 10. Similarly for the evaluation of pH response of the bare CQD solution, it was mixed with different buffers of pH ranging from pH 3 to pH 10. The fluorescence response of the CQD thin film was recorded at an emission wavelength of 484 nm when excited at 365 nm using the fiber optic spectrophotometer (FOS) device.

2.5 Dye sensing studies using the fiber optic spectrophotometer

Calibration curves were obtained for concentrations of different textile dyes ranging between 0 and 100 μM and fluorescence intensities of the CQD thin film based on pH changes. The range of textile dyes was taken according to the permissible limit in water resources. The CQD thin film was dipped in dyes of various concentrations, and the fluorescence of the CQD thin film was recorded with a fiber optic spectrophotometer (FOS) device.

2.6 Dye detection using UV-visible spectrometry and high-performance liquid chromatography (HPLC)

Detection of different dyes in a UV-vis spectrometer was performed at the maximum absorption wavelength. The UV absorption readings at respective λ_{max} values (methyl red, 520 nm; methylene blue, 668 nm; methyl orange, 464 nm; and bromocresol green, 610 nm) for various concentrations of all the dyes were recorded and plotted in calibration curves with absorption at each concentration.

High performance liquid chromatography (HPLC) (Prominence-I LC-2030C, Shimadzu) was performed to detect all dyes at various concentrations within the range of 0–100 μM. Different HPLC methods for the different dyes were used with a common C18 column of 5 μm (4.6 × 250 mm) (Shimadzu, Japan). Methyl red and bromocresol green were analysed using a mobile phase, set in the isocratic mode, composed of acetonitrile and MilliQ water in a 60 : 40 ratio, with detector wavelengths set to 524 nm and 434 nm, respectively, and a flow rate of 0.8 mL min^{-1}. Methyl orange was evaluated using acetonitrile and ammonium acetate in a 60 : 40 ratio having a flow rate of 0.6 mL min^{-1} with a wavelength of 465 nm and for methylene blue, the wavelength was set at 665 nm with the mobile phase comprising methanol and MilliQ in a 70 : 30 ratio with 0.7 mL min^{-1} flow rate.

2.7 Dye spiking studies in river water and household water

Water samples from the Narmada river were taken from Omkareshwar, Khandwa, India, and those from the Kshipra river were taken from Ujjain, India. The spiking studies of all dyes in various matrices of water were performed using all three methods (CQD-based thin film, HPLC and UV-vis). The estimation of concentration of all dyes was calculated using the calibration curves for various matrices of water. Analytical parameters like accuracy, resolution, sensitivity, the limit of detection (LOD), *etc.* were calculated using a spiking experiment for each method. Analytical parameters of all three methods *viz.* CQD-based thin film, HPLC method and UV-

visible-based method, were compared with the objective to test the suitability of the developed sensor against state-of-the-art and sophisticated laboratory instruments.

2.8 Stability of CQD thin films

The CQD-containing thin films were stored at room temperature as CQDs are stable at room temperature and all experiments were carried out at room temperature. In order to evaluate long-term storage stability and photostability, the CQD-based thin films were analysed over a period of 2 months for fluorescence emission signals at frequent intervals.

2.9 Statistical analysis

The Student paired *t*-test and Pearson correlation coefficient (*r*) were calculated and analysed for the significance of experimental data. The *t*-test was performed to determine whether the means of the two groups (real and estimated groups) are equal/similar.

3. Results and discussion

3.1 Synthesis and characterization of CQDs and CQD-containing thin films

The synthesis of folic acid CQDs involved a microwave-assisted one-pot facile method in which folic acid acts as a carbon source. Absence of any passivant in the synthesis of the CQDs provides the advantage of a high quantum yield.[34] The quantum yield was calculated for the synthesized CQDs with quinine sulphate as the reference and found to be around 22%. After synthesis of bare CQDs in the solution phase, the thin film was synthesized by mixing the CQD solution in 5% chitosan solution, as chitosan is a polymer which is used because of its stability between pH 4 and pH8, which is a requirement of dye-sensing strategies.

Synthesized bare CQDs were characterized using a UV-vis spectrometer (UV1900i, Shimadzu, Japan). It was used to analyse the absorption spectra of CQDs: λ_{max} was observed at 365 nm for synthesized CQDs and maximum emission was recorded at 486 nm (blue colour) (Fig. 2A) by using a fiber optic spectrophotometer (FOS) (Flame, Ocean Optics, USA). X-ray photoelectron spectroscopy (XPS) was performed to characterize the chemical composition of the CQDs, and the peaks at 296 eV for C1s and 532 eV for O1s were observed (Fig. 2B). These prominent eV peaks show the presence of mainly 2 elements, carbon and oxygen only, and indicate the presence of bonds comprising only C and O like C–C/C=C, C=O, and C–O–H bonds.[26] For the analysis of the crystalline and lattice parameters, X-ray diffraction (XRD) was performed and the XRD pattern for the synthesized bare CQDs shows a prominent peak at around 27.13°, which indicates the (002) plane with a d-spacing value of 0.38 nm, confirming the nanometre size of the CQDs synthesised (Fig. 2C). The 20–27° value of 2θ indicates the characteristic peak of carbon.[35,36] FTIR analysis was used to identify the functional groups and in folic acid the peaks between 3400 and 3300 cm^{-1} show the presence of the carboxylic group while the synthesized CQD thin film shows peaks between 3480 and 3360 cm^{-1} and at around 2500 cm^{-1} corresponding to the presence of O–H and N–H stretching vibrations, which indicate the presence of carboxylic acid and amine groups as shown in Fig. 2D. Transmission electron microscopy (TEM) was performed for the morphologi-

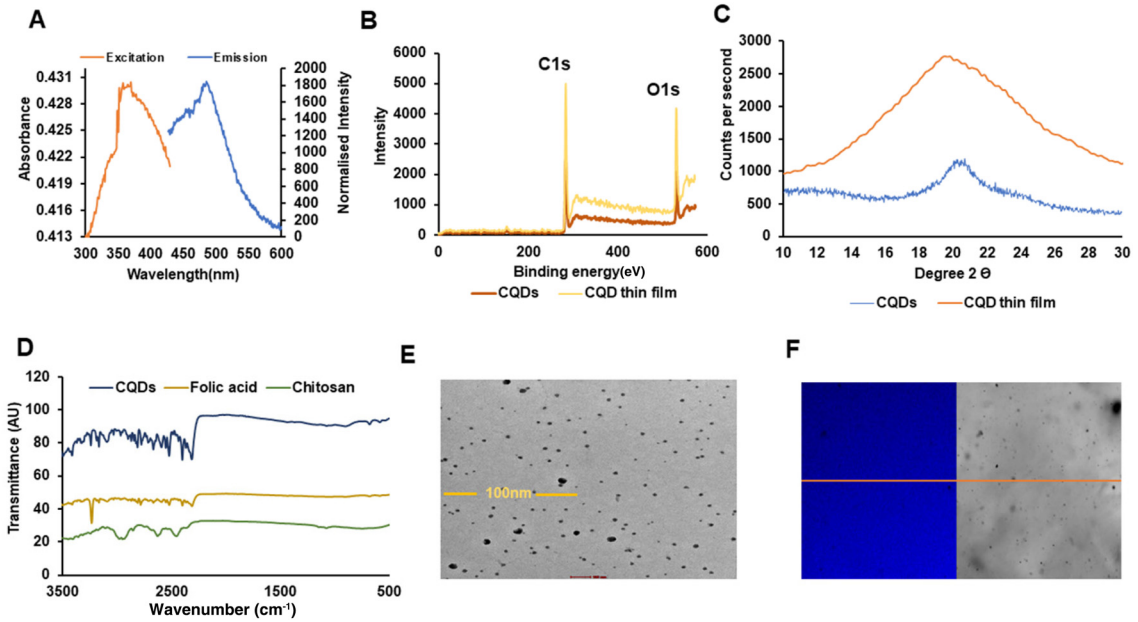

Fig. 2 Characterization of CQDs and CQD-containing films: (A) optical characterization of CQD thin film, (B) X-ray photoelectron spectroscopy (XPS) analysis, (C) X-ray diffraction analysis of CQDs and CQD thin film, (D) FTIR analysis of CQD thin films, folic acid and chitosan, (E) transmission electron microscopy imaging of CQDs and (F) confocal laser scanning microscopy analysis of CQD thin film.

cal and structural characterization of the synthesized bare CQDs, and revealed a more monodispersed distribution with size ranges of 7 ± 4 nm (Fig. 2E). The characterization of CQD thin films was carried out similarly to the bare CQD characterization, and in the optical characterization, λ_{max} was observed at 365 nm for the synthesized CQDs with the maximum emission being recorded at 488 nm (blue colour). Similarly for the chemical analysis, X-ray photoelectron spectroscopy (XPS) was performed and peaks at 294 eV for C1s and 529 eV for O1s were observed. For the analysis of the crystalline and lattice parameters, X-ray diffraction (XRD) was used and the CQD thin films show a prominent peak at around 22.13°, which indicates the (002) plane with a d-spacing value of 0.22 nm. For the evaluation of fluorophore distribution in the CQD thin films, confocal laser scanning microscopy (CLSM) was carried out, which revealed even distribution with constant and uniform fluorescence all over the CQD thin films (Fig. 2F).

All the characterization results of the CQD thin films were found to be comparable with bare CQD characterization results as shown in Fig. 2B and C, while optical spectra and pH data are overlaid with those of bare CQDs shown in Fig S1†, which indicate that the characteristic properties of CQDs remain the same after formation of CQD thin films without any interference.

All textile dyes, which are the analytes for detection with the CQD thin film, have fluorescence emission along with their respective excitation. With the aim being to check any interference of excitation–emission of these dyes using CQDs/CQD-loaded thin films, we recorded the excitation and emission values of all dyes and CQDs and it was observed that CQD thin films have excitation (λ_{max}) at around 365 nm, which was found to be different from those of all the textile dyes: methyl red (530 nm), methyl orange (470 nm), methylene blue (665 nm) and bromocresol green (596 nm), as shown in Fig. 3A. The emission of CQDs was found to be around 484 nm, which was found to be different from those of all dye analytes: methyl red (625 nm), methyl orange (605 nm), methylene blue (702 nm), and bromocresol green (590 nm), as shown in Fig. 3B. The excitation and emission values of all dyes were found to be different from that of the CQDs thin film, which indicates that there is no interference of these textile dyes on the optical properties of CQD thin films. The absorbance and fluorescence emission spectra clearly indicate that the peak intensities of dyes do not act as interference for the CQD response.

3.2 Evaluation of pH sensitivity of synthesized CQDs and CQD thin films

The pH sensitivity of the bare CQD solution and CQD-loaded thin films was evaluated by exposing them to various pH buffers in the range of pH 3–10. An increase of pH and therefore basicity means the number of OH^- ions increases and these bind to the CQD shells, and due to this phenomenon, the fluorescence of CQDs increases as shown in Fig. 5A. In a similar fashion, CQD thin films also show an increase in fluorescence as the pH increases from pH 3 to pH 10 as shown in Fig. 5B. This indicates that the synthesized CQDs have pH-sensitive properties as revealed in Fig. 5B, and that the pH-sensitive properties are retained in the CQD-loaded thin film. The sensitivity of the fluorescence response was comparable in both CQDs (0.067/unit of pH) and CQD-loaded thin films (0.076/unit of pH). The pH profile indicates the suitability of CQDs for the estimation of pH in an analyte. The pH response of the CQD thin films was also compared with that of bare or pure chitosan thin films, as shown in Fig. 5C. It was observed that there is no upward trend of fluorescence response in the bare or pure chitosan thin film with increasing pH as is observed in the CQD thin films with increasing pH.

3.3 Stability of CQD thin films

To evaluate the photostability of CQD thin films, the fluorescence of CQDs was recorded through a fiber optic spectrophotometer (FOS) device at regular intervals for over 2 months. It was found that the CQD thin films were photostable with minimal photobleaching (<20% of initial fluorescence intensity) as indicated in Fig. 5D.

3.4 Dye-sensing studies using CQD thin films

The pH-sensitive property of CQD-loaded thin films is used for the detection of textile dyes in various water samples. All tested dyes have pH-changing ability such that methyl red dye is an acidic dye having a quinonoid structure with pK_a value of

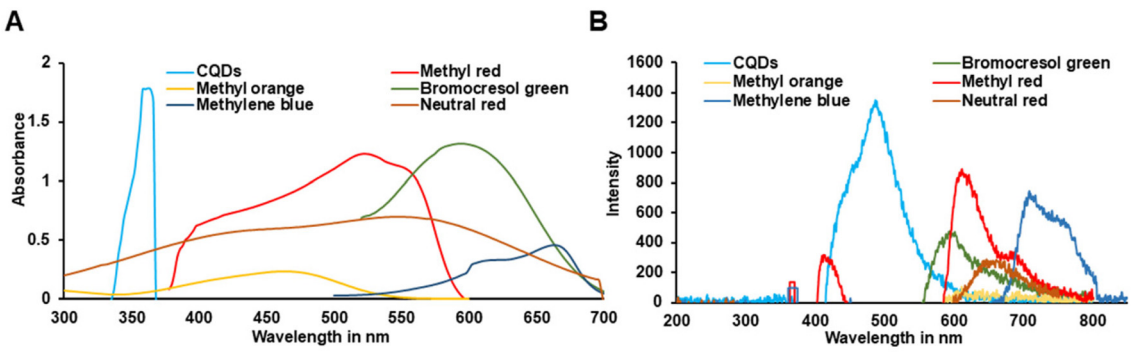

Fig. 3 Overlay of (A) absorption of CQDs and methyl red, bromocresol green, methyl orange, methylene blue and neutral red dyes, (B) fluorescence emission of CQDs with methyl red, bromocresol green, methyl orange, methylene blue and neutral red dyes.

5.1 along with a pH range of pH 4.2–6.3, and is soluble in acetone. Second, methyl orange is an acidic dye but has a sodium sulfonate-based structure having a pH range between 3.1 and 4.4 along with pK_a value of 3.47 and is soluble in water. Bromocresol dye is also an acidic dye with a triphenylmethane structure having pK_a value of 4.90 along with a pH range of 3.8–5.4, and is soluble in water. Of the four dyes selected as analytes, methylene blue is a basic dye having a thiazine structure with a pH range of 6–8 and is mainly soluble in acetone. Due to all described properties of these dyes, the presence of any one of these dyes will change the pH of its matrix.

This pH change in the environment is detected by the synthesized CQD thin films, which will provide a change in the fluorescence response. Calibration curves were plotted with different concentrations (0–100 μM), as per the permissible range of all four textile dyes, *i.e.* methyl red, methyl orange, bromocresol green, and methylene blue, from their fluorescence emission values.

The sensing mechanism of the synthesized CQD thin films was based on the acidic and basic nature of dyes. Acidic dyes have H^+/protons present that withdraw electrons from the CQDs, which results in the loss of electrons from the CQDs and a decrease in the fluorescence of the CQD thin film occurs, while in the presence of basic dyes, which contain OH^- ions that provide electrons to the CQDs, the addition of electrons in the CQDs causes the fluorescence of the CQD thin film to increase, as shown in Fig. 4.

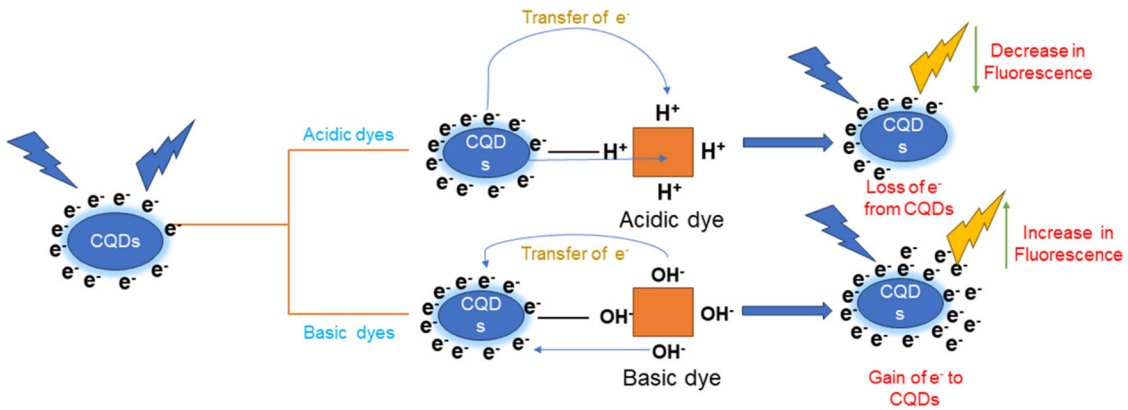

Fig. 4 Mechanism of sensing of dyes with the CQD thin-film-based sensor.

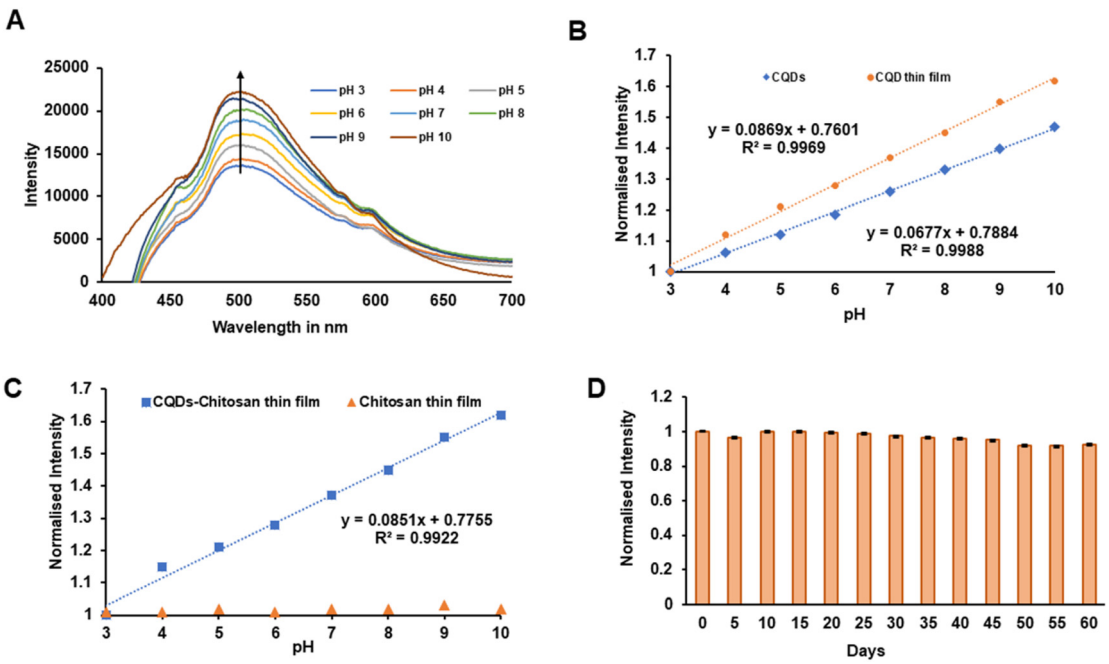

Fig. 5 The pH response of synthesized CQD thin films: (A) overlay spectra, (B) linear curve of CQDs and CQD thin film, (C) pH responses of CQD–chitosan and pure chitosan thin films, (D) photostability of CQD thin film.

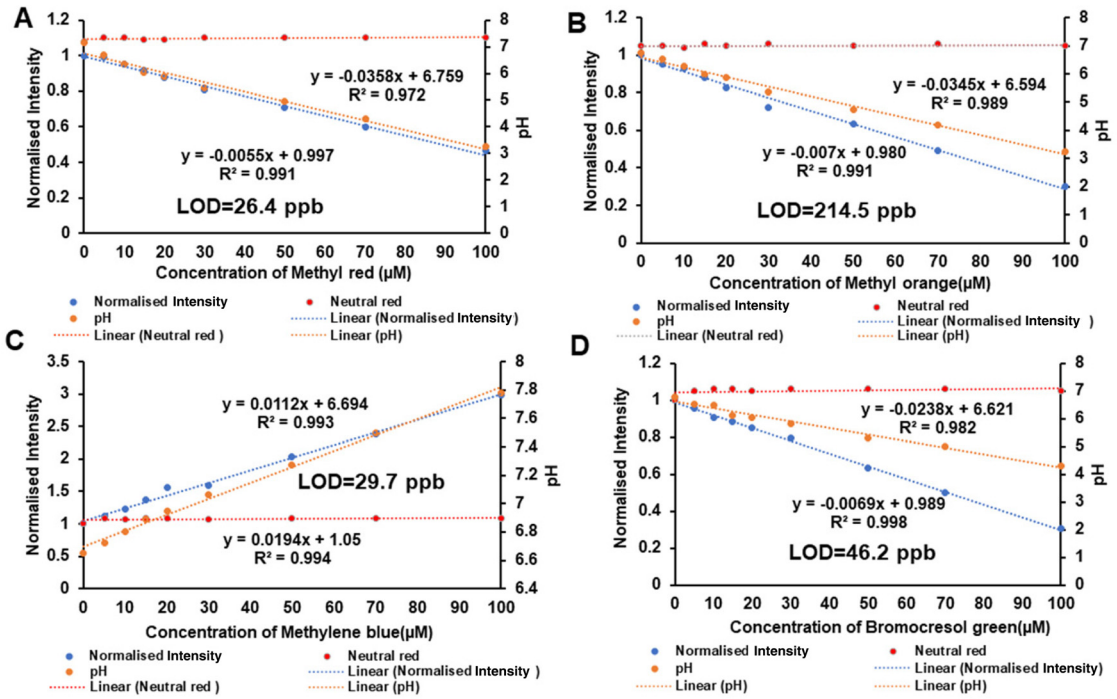

Fig. 6 Calibration curves of detection of (A) methyl red, (B) methyl orange, (C) methylene blue and (D) bromocresol green in the range of 0–100 μM with CQD thin-film-based detection. The pH changes are described on secondary axes of each graph (A–D) and neutral red dye was used as a reference dye along with all the dyes for calibration curves (A–D).

The calibration curves were found to be linear with a decreasing trend in the cases of three of the dyes, namely methyl red (Fig. 6A), methyl orange (Fig. 6B) and bromocresol green (Fig. 6D), as they are all acidic dyes and the pH decreases with an increase of concentration of these three dyes. In the case of methylene blue (Fig. 6C), the calibration curve was found to be linear with an increasing trend as methylene blue is a basic dye, and the pH increases with an increase in the concentration of methylene blue.

The pH values of all dyes were also plotted on the secondary axis along with the respective calibration curve. Neutral red dye is a textile dye having neutral pH, and thus it was used as the reference dye for the detection of other dyes. A straight line with minimal slope was observed due to the neutral pH properties of neutral red dye making it a suitable dye as the reference for estimation of other acidic/basic dyes that show an increasing/decreasing trend of fluorescence emission, respectively.

The CQD thin-film fluorescence intensity response for all four dyes shows a linear regression equation: $y = -0.0055x + 0.9974$ for methyl red, $y = -0.007x + 0.9898$ for methyl orange, $y = 0.0194x + 1.0507$ for methylene blue and $y = -0.0069 + 0.9894$ for bromocresol green. The ratio of the intensity changes per unit change of concentration of dye was used to calculate the sensitivity of the sensors.

The sensitivity was found to be 0.0055 per unit of intensity change per unit micromolar concentration change in methyl red with $R^2 = 0.991$; for methyl orange, the sensitivity was 0.007/μM with $R^2 = 0.991$; similarly, for bromocresol green and methylene blue, the sensitivity along with R^2 was 0.0069/μM with $R^2 = 0.998$ and 0.019/μM with $R^2 = 0.994$, respectively.

With respect to sensitivity, methylene blue shows the highest sensitivity among all four dyes. The sensitivity of the sensor to basic dyes is greater as compared to that for acidic dyes because as the pH increases towards basicity, the fluorescence increases and the sensitivity of the sensor in terms of the slope of the calibration curve is greater. Similarly, in the case of sensing acidic dyes, as the concentration of acidic dyes increases the pH moves towards the acidic range and decreases and due to this the fluorescence of the CQD thin films decreases, which decreases the slope of the trendline equation of the calibration curve and sensitivity decreases.

On hydrolysis of the acidic dyes methyl red, methyl orange and bromocresol green, according to the structure of these dyes as shown in Fig. S5,† H^+ ions or protons are released, which upon contacting with the CQDs of the CQD-loaded thin film withdraw electrons from the CQDs, due to which quenching of the CQDs occurs and results in a decrease of fluorescence of the CQD-loaded thin film. On the other hand, on hydrolysis of basic dyes, such as methylene blue, due to the complex structure as shown in Fig. S5,† OH^- ions are released that bind with the CQD electrons and strengthen the shells of the CQDs, which increases the fluorescence of the CQD-loaded thin films.

The specificity of the slope was analysed by comparing the slope value of each calibration curve equation of all dyes as

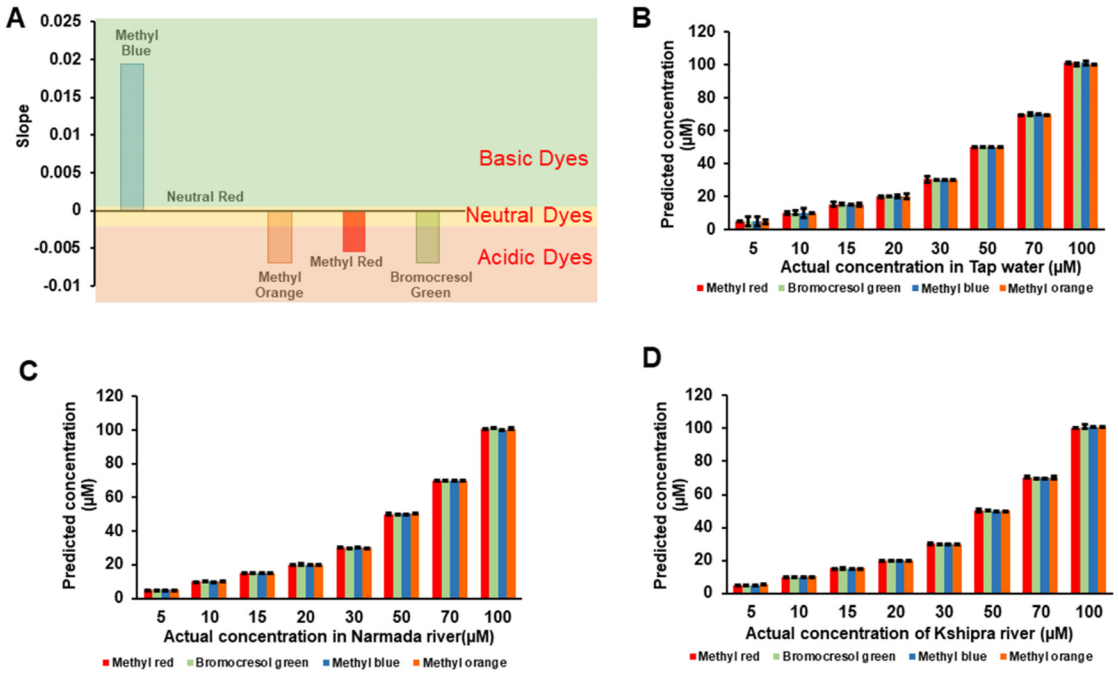

Fig. 7 (A) Comparison of slope values of different dyes, and (B, C and D) spiking studies of CQD thin-film-based detection of dyes in household tap water, Narmada river water and Kshipra river water, respectively.

shown in Fig. 7A. It is found that the acidic dyes have negative slope values, such as methyl red, which has a slope value of −0.0055 units per μM. Similarly methyl orange (−0.007 units per μM) and bromocresol green (−0.0069 units per μM) have negative slope values, whereas basic dyes have positive slope values, such as that of methylene blue, which has a slope value of 0.019 units per μM. This analysis will help identify unknown samples of dyes.

In terms of pH, the change in the pH range is found to be greatest in methyl red as it is the strongest acidic dye among all four dye analytes having pH decreases in the range of pH 6 to pH 3, followed by methyl orange (pH 6 to pH 3.3), bromocresol green (pH 6.2 to pH 4.2), and the smallest change was observed in methylene blue as it is a basic dye where the pH is observed to increase from pH 6.8 to pH 7.8.

3.5 Spiking studies in household water and river water

Three different matrices of water were used for the spiking studies, mainly household tap water and two matrices from river water (Narmada and Kshipra rivers). Different concentrations of all dyes were spiked in these three matrices separately and brought into contact with CQD thin films for sensing. Spiking studies and fluorescence of CQD thin films were employed to check the suitability of CQD thin film-based sensors for the detection of textile dyes in water matrices.

The accuracy of the sensing mechanism was observed in terms of percentage recovery values from spiking studies. In tap water (Fig. 7B), with CQD-loaded thin films, for methyl red, the accuracy in terms of % recovery was calculated from eqn (S3)† and found to be 101.36% with a minimal error of 1.36%. Similar values were obtained for bromocresol green (100.91% ± 0.91%), methyl orange (100.70% ± 0.70%) and methylene blue (100.78% ± 0.78%). After attaining improved and better percentages of recovery than those in previous methods with tap water, the spiking studies in river water samples were also carried out with all the dyes. In Narmada river samples (Fig. 7C), the percentage recovery in terms of accuracy was observed in methyl red at 100.75% with a mean error of 0.75%. Similar values were found for methyl orange (101.03% ± 1.03%), bromocresol green (100.86% ± 0.86%), and methylene blue (100.70% ± 0.70%). In a similar fashion, in the water samples from the Kshipra river (Fig. 7D), the accuracy in terms of the % recovery was determined for bromocresol green as 100.78% with a mean error of 0.78%. Similar values for methyl red (100.84% ± 0.84%), methylene blue (100.72% ± 0.72%), and methyl orange (101.41% ± 1.41%) were obtained. The percentage recovery in terms of accuracy was determined to be good and values were all around 100% in the spiking studies in all three water matrices, which shows the better suitability of the CQD thin-film-based sensor in all three water matrices for all four textile dyes.

A combination of multiple acidic dyes or a combination of multiple basic dyes can very well be detected using the developed CQD thin-film-based sensor. The only limitation where the sensor might not work is when the combination of acidic and basic dyes in a single real sample leads to a neutral pH. Small modifications (*e.g.* use of a secondary light source and sequential analysis will negate false positives coming from solutions like alkaline/acidic water of pH 8/pH 4 and analysis at different wavelengths other than 500 nm) in instrumenta-

tion along with the developed sensor films will aid in the identification of different types of dyes present in water resources.

Alternatively, since the dyes used in the study are also fluorescent in nature, a secondary light source, which can be sequentially operated after the first measurement using CQDs, can be used. Using the second light source, a secondary emission peak will emerge corresponding to the emission of the dyes.

3.6 Dye detection and spiking studies using UV-visible spectrometry and HPLC

With the aim of comparing the sensing data of CQD thin-film-based detection of dyes with data from standard instruments, we carried out the detection of dyes using a UV-vis spectrometer.

In UV-vis-based detection, the spectra of all dyes are recorded to find out the λ_{max} of the respective dyes. The UV spectra of the dyes indicate λ_{max} of the dyes as follows: for methylene blue λ_{max} was found at 664 nm; for methyl orange, 464 nm; bromocresol green, 434 nm; and for methyl red, 524 nm. The absorption of different concentrations of dyes in DI water was recorded at their respective maximum wavelengths. The calibration curves of all dyes were plotted in the 0–100 μM concentration range. The calibration curves of all dyes were found to be linear, as shown in Fig. S2.†

A comparison of CQD thin-film-based detection with highly sophisticated instruments, such as HPLC-based detection, of all four textile dyes was done. The concentration of dyes was in the range of 0–100 μM. The retention time for methyl red was found at 7.87 minutes, for bromocresol green it was 3.97 minutes, for methyl orange it was 5.60 minutes and for methylene blue it was 4.977 minutes, as shown in Fig. S2.† All calibration curves of all dyes with HPLC were found to be linear as, shown in Fig. S3.†

In spiking studies of dyes in three matrices of water (household tap water, and Narmada and Kshipra river samples), the accuracy in terms of the percentage recovery in both UV-vis- and HPLC-based detection was also found to be around 100% with minimal average errors of 3–5% as in CQD thin-film-based detection, as shown in Fig. 8. The sensing parameters of both these methods (CQD thin film with UV-vis and HPLC) are compared.

3.7 Comparison of analytical paramerters of all three dye detection methods

The comparison CQD thin-film-based detection with standard instrument-based detection, *i.e.* UV-vis spectrometry and HPLC, is presented in Table 1. The accuracy in terms of the

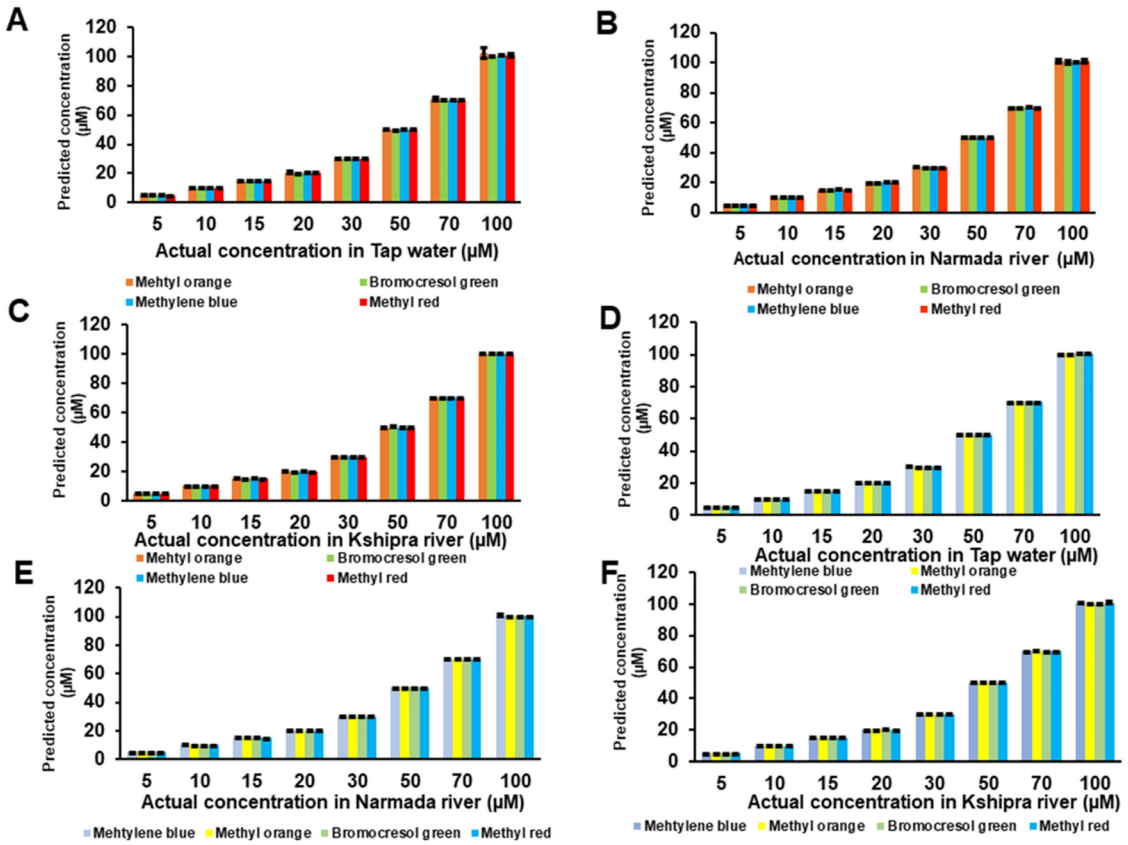

Fig. 8 Spiking studies of UV-vis spectrometer-based detection of dyes in (A) tap water, (B) Narmada river water, and (C) Kshipra river water, and spiking studies of HPLC-based detection of dyes in (D) tap water, (E) Narmada river water, and (F) Kshipra river water.

Table 1 Comparison of analytical parameters of detection of dyes with CQD thin-film-based and standard methods

	Methyl red			Methyl orange			Bromocresol green			Methylene blue		
Analytical Parameters	CQD thin film	UV-vis	HPLC	CQD thin film	UV-vis	HPLC	CQD thin film	UV-vis	HPLC	CQD thin film	UV-vis	HPLC
Accuracy												
Tap water	101.3%	100.6%	100.8%	100.7%	100.3%	101.7%	100.9%	100.3%	100.4%	100.7%	100.4%	100.6%
Narmada river	100.7%	100.6%	100.6%	101.1%	100.6%	100.4%	100.8%	100.6%	100.4%	100.7%	100.8%	100.7%
Kshipra river	100.8%	100.7%	100.6%	101.4%	100.5%	100.8%	100.7%	100.7%	100.5%	100.7%	100.3%	100.8%
Linear regression	0.991	0.997	0.998	0.991	0.999	0.998	0.998	0.994	0.998	0.991	0.999	0.998
Response time (in minutes)	1	2–3	7.87	1	2–3	5.60	1	3.97	2–3	1	2–3	4.77
Sensitivity (μM)	0.0055	0.0047	0.74	0.007	0.0022	8.041	0.0069	0.023	2.71	0.0019	0.0049	0.390
Limit of detection (LOD)	26.4 ppb	264 ppb	6.6 ppb	214.5 ppb	66 ppb	8.25 ppb	46.2 ppb	16.5 ppb	9.9 ppb	29.7 ppb	36.3 ppb	23.1 ppb
Limit of quantification (LOQ)	79.2 ppb	792 ppb	19.8 ppb	643.5 ppb	198 ppb	24.75 ppb	138.6 ppb	49.5 ppb	29.7 ppb	89.1 ppb	108.9 ppb	69.3 ppb
Resolution (in ppb)	8	80	2	65	20	2.5	14	5	3	9	11	7

percentage recovery of CQD thin-film-based detection was found to be similar and comparable with that of UV-vis- and HPLC-based detection. For the linearity of all dyes in terms of the regression coefficient (R^2), CQD thin-film-based detection has similar and comparable linearity with that of both standard methods (HPLC and UV-vis), which is above 0.99 indicating high significance. The response time of detection of dyes is much lower in CQD thin-film-based detection and is around 5- to 6-fold lower than in HPLC and 1- to 2-fold lower than in UV-vis-based detection. This indicates that CQD-based thin films have potential for detection in response times shorter than those of HPLC and UV-vis-based detection. The sensitivity of the sensing mechanism, which was revealed by the regression equation, was higher in HPLC for all dyes as it is a highly sophisticated technique. The sensitivity with UV-vis-based detection is high as compared with CQD thin-film-based detection in three dyes, *i.e.* methyl red, methyl orange and bromocresol green, and lower in the case of methylene blue. The sensitivity of HPLC is 157- and 136-fold greater than that of CQD thin-film- and UV-vis-based detection of methyl red, respectively. Similarly, for methyl orange, HPLC sensitivity was 3655- and 1148-fold higher, for bromocresol green it was 117.8-fold and 392-fold greater, and for methylene blue it was 79.5-fold and 205.8-fold higher than the sensitivity of UV-vis- and CQD thin-film-based detection, respectively. Most of the sensitivity, LOD, and LOQ values were superior using the HPLC method, which was obviously predicted considering the sophisticated nature of the HPLC instrument. However, considering economic reasons, HPLC cannot be used for on-site detection. Overall the LOD and LOQ of the sensing mechanism are comparable with respect to CQD thin-film-based and UV-vis detection, while they are better in the case of HPLC-based detection. CQD-based thin films were able to show the best LOD for methylene blue and methyl red to an extent of being 1.25 10 times better in comparison with their UV-vis counterparts. On the other hand, the CQD-loaded thin films showed the best sensitivity for methyl red, methyl orange and bromocresol green, which were 1.17–3.18 times better than that from the UV-vis method. Furthermore, it was found that HPLC, being a sophisticated instrument for detection, showed excellent results in terms of low LODs for almost all dyes.

The LOD of HPLC-based detection was 10-fold and 4-fold lower for methyl red as compared to UV-vis- and CQD-based detection, respectively, and CQD thin films have 10-fold lower detection as compared to UV-vis-based detection, while for methyl orange it was 8-fold and 26-fold lower, for bromocresol green, 2-fold and 5-fold lower, and for methyl blue, 1.5-fold lower and the same LOD as compared to UV-vis- and CQD-based detection, respectively. This suggests that CQD thin-film-based detection has comparable LOD and LOQ with respect to the UV-vis- and HPLC-based detection methods with ppb detection capabilities. The resolution of HPLC is better, and other than that the CQD thin film and UV-vis spectrometer have comparable resolution.

The comparison of analytical parameters shows that CQD thin-film-based detection of the dyes has good sensitivity, better resolution and good ppb LODs, and is comparable to standard instruments used in UV-vis spectrometry. The CQD thin films can be used for point-of-care and on-site detection of dyes in different matrices of water and are able to replace standard instruments, which are expensive, less portable and require complex sample preparation, for real-time monitoring and detection of dyes.

4. Conclusion

This study demonstrates the application of the pH-sensitive property of folic acid CQD thin-film-based sensors for the detection of textile dyes in different matrices of water. The

presence of dyes causes changes in the pH of the water matrices corresponding to the nature of the dyes (acidic, basic or neutral). The changes in pH can be detected using folic acid CQD thin films. The analytical parameters of sensing studies involving CQD thin-film-based detection are compared with those of sophisticated instruments, such as HPLC. CQD thin-film-based sensing uses fiber optic spectrometric measurements, which are able to show the point-of-use approach for the detection of dyes in water in real-time monitoring with a response time of 1 minute. The results show that the CQD thin-film sensor can be used for pH-sensitive detection of all dyes that are chemically acidic or basic in nature using a portable approach so that it can be substituted for highly expensive and high-end analytical equipment.

Author contributions

Vyas T. performed all the experiments and data analysis. Vyas T. and Joshi A. compiled the data and wrote the manuscript. Joshi A. and Gogoi M. were involved in proofreading of the manuscript.

Conflicts of interest

The author declares no conflict of interest.

Acknowledgements

This work was supported by the Prime Minister Research Fellowship (PMRF) (grant no. 2101309) and Department of Biotechnology, GOI-NER project (grant no. BT/PR24652/NER/795/2017). T. V. acknowledges financial support from the Prime Minster Research Fellowship (PMRF). A. J. and M. G. acknowledge DBT-NER project BT/PR24652/NER/795/2017. A. J. acknowledges DST FIST Project No. SR/FST/LS-I/2020/62.

References

1 R. G. Saratale, G. D. Saratale, J. S. Chang and S. P. Govindwar, Bacterial decolorization and degradation of azo dyes: A review, *J. Taiwan Inst. Chem. Eng.*, 2011, **42**(1), 138–157, DOI: **10.1016/j.jtice.2010.06.006**.

2 J. Kiernan, Classification and naming of dyes, stains and fluorochromes, *Biotech. Histochem.*, 2001, **76**(5–6), 261–278, DOI: **10.1080/bih.76.5-6.261.278**.

3 M. Adeel, M. M. Rahman, I. Caligiuri, V. Canzonieri, F. Rizzolio and S. Daniele, Recent advances of electrochemical and optical enzyme-free glucose sensors operating at physiological conditions, *Biosens. Bioelectron.*, 2020, **165**, 112331, DOI: **10.1016/j.bios.2020.112331**.

4 I. Ayadi, Y. Souissi, I. Jlassi, F. Peixoto and W. Mnif, Chemical Synonyms, Molecular Structure and Toxicological Risk Assessment of Synthetic Textile Dyes: A Critical Review, *J. Dev. Drugs*, 2016, **5**, 57, DOI: **10.4172/2329-6631.1000151**.

5 E. Rápó and S. Tonk, Factors Affecting Synthetic Dye Adsorption; Desorption Studies: A Review of Results from the Last Five Years (2017–2021), *Molecules*, 2021, **26**(17), 5419, DOI: **10.3390/molecules26175419**.

6 H. Pan, J. Feng, G.-X. He, C. E. Cerniglia and H. Chen, Evaluation of impact of exposure of Sudan azo dyes and their metabolites on human intestinal bacteria, *Anaerobe*, 2012, **18**(4), 445–453, DOI: **10.1016/j.anaerobe.2012.05.002**.

7 F. Colakoglu and M. L. Selcuk, The Embryotoxic Effects of in Ovo Administered Sunset Yellow FCF in Chick Embryos, *Vet. Sci.*, 2021, **8**(2), DOI: **10.3390/vetsci8020031**.

8 K. Hamada, H. Nonogaki, Y. Fukushima, B. Munkhbat and M. Mitsuishi, Effects of hydrating water molecules on the aggregation behavior of azo dyes in aqueous solutions, *Dyes Pigm.*, 1991, **16**(2), 111–118, DOI: **10.1016/0143-7208(91)85003-Q**.

9 Markandeya, D. Mohan and S. P. Shukla, Hazardous consequences of textile mill effluents on soil and their remediation approaches, *Clean. Eng. Technol.*, 2022, **7**, 100434, DOI: **10.1016/j.clet.2022.100434**.

10 J. Yang, C. Gomes da Rocha, S. Wang, A. A. Pupim Ferreira and H. Yamanaka, A label-free impedimetric immunosensor for direct determination of the textile dye Disperse Orange 1, *Talanta*, 2015, **142**, 183–189, DOI: **10.1016/j.talanta.2015.04.042**.

11 S. Bonan, G. Fedrizzi, S. Menotta and C. Elisabetta, Simultaneous determination of synthetic dyes in foodstuffs and beverages by high-performance liquid chromatography coupled with diode-array detector, *Dyes Pigm.*, 2013, **99**(1), 36–40, DOI: **10.1016/j.dyepig.2013.03.029**.

12 T. Rasheed, M. Bilal, H. M. N. Iqbal, H. Hu and X. Zhang, Reaction Mechanism and Degradation Pathway of Rhodamine 6G by Photocatalytic Treatment, *Water, Air, Soil Pollut.*, 2017, **228**(8), 291, DOI: **10.1007/s11270-017-3458-6**.

13 S. Singh, A. Kumar and H. Gupta, Activated banana peel carbon: a potential adsorbent for Rhodamine B decontamination from aqueous system, *Appl. Water Sci.*, 2020, **10**(8), 185, DOI: **10.1007/s13201-020-01274-4**.

14 J. R. Richardson, V. Fitsanakis, R. H. S. Westerink and A. G. Kanthasamy, Neurotoxicity of pesticides, *Acta Neuropathol. (Berl.)*, 2019, **138**(3), 343–362, DOI: **10.1007/s00401-019-02033-9**.

15 L. Rafaëlly, S. Héron, W. Nowik and A. Tchapla, Optimisation of ESI-MS detection for the HPLC of anthraquinone dyes, *Dyes Pigm.*, 2008, **77**(1), 191–203, DOI: **10.1016/j.dyepig.2007.05.007**.

16 R. M. Birch, C. O'Byrne, I. R. Booth and P. Cash, Enrichment of Escherichia coli proteins by column chromatography on reactive dye columns, *Proteomics*, 2003, **3**(5), 764–776, DOI: **10.1002/pmic.200300397**.

17 J. Jiao, *et al.*, Simultaneous determination of three azo dyes in food product by ion mobility spectrometry,

J. Chromatogr. B, 2016, **1025**, 105–109, DOI: 10.1016/j.jchromb.2016.05.002.

18 F. Turak, M. Dinç, Ö. Dülger and M. U. Özgür, Four Derivative Spectrophotometric Methods for the Simultaneous Determination of Carmoisine and Ponceau 4R in Drinks and Comparison with High Performance Liquid Chromatography, *Int. J. Anal. Chem.*, 2014, e650465, DOI: 10.1155/2014/650465.

19 S. Mishra, R. P. Singh, C. C. Rath and A. P. Das, Synthetic microfibers: Source, transport and their remediation, *J. Water Process Eng.*, 2020, **38**, 101612, DOI: 10.1016/j.jwpe.2020.101612.

20 R. L. C. Voeten, I. K. Ventouri, R. Haselberg and G. W. Somsen, Capillary Electrophoresis: Trends and Recent Advances, *Anal. Chem.*, 2018, **90**(3), 1464–1481, DOI: 10.1021/acs.analchem.8b00015.

21 J. Bhattacharjee, S. Mishra and A. P. Das, Recent Advances in Sensor-Based Detection of Toxic Dyes for Bioremediation Application: a Review, *Appl. Biochem. Biotechnol.*, 2022, **194**(10), 4745–4764, DOI: 10.1007/s12010-021-03767-7.

22 S. Dolai, S. K. Bhunia, S. Rajendran, V. UshaVipinachandran, S. C. Ray and P. Kluson, Tunable fluorescent carbon dots: synthesis progress, fluorescence origin, selective and sensitive volatile organic compounds detection, *Crit. Rev. Solid State Mater. Sci.*, 2021, **46**(4), 349–370, DOI: 10.1080/10408436.2020.1830750.

23 P. Devi, P. Rajput, A. Thakur, K.-H. Kim and P. Kumar, Recent advances in carbon quantum dot-based sensing of heavy metals in water, *TrAC, Trends Anal. Chem.*, 2019, **114**, 171–195, DOI: 10.1016/j.trac.2019.03.003.

24 X. Wu, *et al.*, Carbon quantum dots as fluorescence resonance energy transfer sensors for organophosphate pesticides determination, *Biosens. Bioelectron.*, 2017, **94**, 292–297, DOI: 10.1016/j.bios.2017.03.010.

25 I. Walton, *et al.*, A Fluorescent Dipyrrinone Oxime for the Detection of Pesticides and Other Organophosphates, *Org. Lett.*, 2012, **14**(11), 2686–2689, DOI: 10.1021/ol300799f.

26 S. Choudhary, B. Joshi and A. Joshi, Translation of Carbon Dot Biosensors into an Embedded Optical Setup for Spoilage and Adulteration Detection, *ACS Food Sci. Technol.*, 2021, **1**, 1068–1076, DOI: 10.1021/acsfoodscitech.1c00089.

27 S. Dolai, S. K. Bhunia and R. Jelinek, Carbon-dot-aerogel sensor for aromatic volatile organic compounds, *Sens. Actuators, B*, 2017, **241**, 607–613, DOI: 10.1016/j.snb.2016.10.124.

28 Y. Liu, H. Huang, W. Cao, B. Mao, Y. Liu and Z. Kang, Advances in carbon dots: from the perspective of traditional quantum dots, *Mater. Chem. Front.*, 2020, **4**(6), 1586–1613, DOI: 10.1039/D0QM00090F.

29 A. Kelarakis, Graphene quantum dots: In the crossroad of graphene, quantum dots and carbogenic nanoparticles, *Curr. Opin. Colloid Interface Sci.*, 2015, **20**(5), 354–361, DOI: 10.1016/j.cocis.2015.11.001.

30 H. Liu, J. Ding, K. Zhang and L. Ding, Construction of biomass carbon dots based fluorescence sensors and their applications in chemical and biological analysis, *TrAC, Trends Anal. Chem.*, 2019, **118**, 315–337, DOI: 10.1016/j.trac.2019.05.051.

31 Y. Hu and Z. Gao, Sensitive detection of Sudan dyes using tire-derived carbon dots as a fluorescent sensor, *Spectrochim. Acta, Part A*, 2020, **239**, 118514, DOI: 10.1016/j.saa.2020.118514.

32 M. Tian, *et al.*, Preparation of sulphuric acid-mediated N,S-codoped red emissive carbon dots: Applications in food dyes detection, solid-state luminescence and cell imaging, *Spectrochim. Acta, Part A*, 2022, **281**, 121581, DOI: 10.1016/j.saa.2022.121581.

33 F. Du, F. Zeng, Y. Ming and S. Wu, Carbon dots-based fluorescent probes for sensitive and selective detection of iodide, *Microchim. Acta*, 2013, **180**(5), 453–460, DOI: 10.1007/s00604-013-0954-2.

34 L. Wang, Y. Yin, A. Jain and H. S. Zhou, Aqueous Phase Synthesis of Highly Luminescent, Nitrogen-Doped Carbon Dots and Their Application as Bioimaging Agents, *Langmuir*, 2014, **30**, 14270–14275, DOI: 10.1021/la5031813.

35 X. Zheng, L. Wang, L. Qi and Z. Dong, A Novel Organophosphorus Acid Anhydrolase from Deep Sea Sediment with High Degradation Efficiency for Organophosphorus Pesticides and Nerve Agent, *Microorganisms*, 2022, **10**(6), 1112, DOI: 10.3390/microorganisms10061112.

36 K. Asghar, M. Qasim and D. Das, One-pot green synthesis of carbon quantum dot for biological application, *AIP Conf. Proc.*, 2017, **1832**, 050117, DOI: 10.1063/1.4980350.